JACS
JOURNAL OF THE AMERICAN CHEMICAL SOCIETY

COMMUNICATION

pubs.acs.org/JACS

Quasiemulsion-Templated Formation of α-Fe_2O_3 Hollow Spheres with Enhanced Lithium Storage Properties

Bao Wang,[†,‡,§] Jun Song Chen,[†,‡,§] Hao Bin Wu,[†] Zhiyu Wang,[†] and Xiong Wen (David) Lou*[,†,‡]

[†]School of Chemical and Biomedical Engineering, Nanyang Technological University, 70 Nanyang Drive, Singapore 637457

[‡]Energy Research Institute@NTU, Nanyang Technological University, 50 Nanyang Drive, Singapore 637553

Supporting Information

ABSTRACT: α-Fe_2O_3 hollow spheres with sheet-like subunits are synthesized by a facile quasiemulsion-templated method. Glycerol is dispersed in water to form oil-in-water quasiemulsion microdroplets, which serve as soft templates for the deposition of the α-Fe_2O_3 shell. When tested as anode materials for lithium-ion batteries, these α-Fe_2O_3 hollow spheres manifest greatly enhanced Li storage properties.

Lithium-ion batteries (LIBs), a fast-developing technology in electric energy storage, are the dominant power source for a wide range of portable electronic devices.[1−3] Graphite, the anode material currently used in commercial LIBs, has a relatively low Li storage capacity of 370 mA h g^{-1}. Thus, the search for alternative anode materials has become an urgent task in building the next-generation LIBs, so as to meet the ever-growing performance demands.[3] α-Iron oxide (α-Fe_2O_3), an important member of the metal oxide family, is believed to be a promising candidate to replace graphite because of its much higher theoretical capacity of ~1000 mA h g^{-1}, nontoxicity, and abundance. To date, α-Fe_2O_3 has been widely studied as the anode material for LIBs,[4−14] and the storage of Li is mainly achieved through the conversion reaction between Li^+ and α-Fe_2O_3. Despite of these attractive features, α-Fe_2O_3 suffers from poor cyclability that is associated with the large volume change during charge−discharge.[9] To improve the Li storage capability, different α-Fe_2O_3 nanomaterials with unique structures, including porous particles,[6,10] nanorods or nanotubes,[4,9,14] and hollow particles,[12,13] have been investigated. However, there has been limited success in producing well-defined hierarchical hollow structures of α-Fe_2O_3 with excellent Li storage capabilities.[10,15−18]

Emulsion microdroplets, under the category of soft templates,[19] have been intensively applied to generate hollow nanostructures with a wide range of chemical compositions, including polymers, metals, and metal oxides.[20−30] As compared to hard templates, these soft templates offer distinct advantages because they are generally highly deformable and easily removable.[25] In this work, we report an interesting quasimicroemulsion-templated hydrothermal method to synthesize α-Fe_2O_3 hollow spheres. When applied as the anode material for LIBs, the as-prepared α-Fe_2O_3 hollow spheres exhibit greatly enhanced Li storage properties, with a reversible capacity of as high as 710 mA h g^{-1}, even after 100 charge−discharge cycles.

Figure 1 illustrates the formation process of the α-Fe_2O_3 hollow spheres. In this synthesis, glycerol is first mixed with water

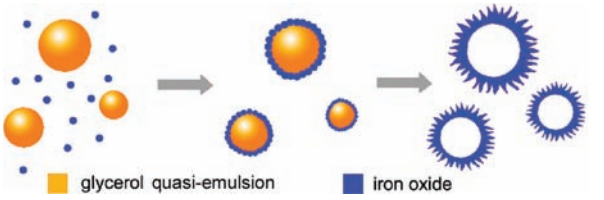

Figure 1. Schematic illustration of the formation of α-Fe_2O_3 hierarchical hollow spheres.

to form a uniform quasimicroemulsion. Even though glycerol and water are miscible under thermodynamic equilibrium, it is shown that these polar solutes, like 2-propanol or acetone, have the tendency to self-aggregate in the aqueous medium, thus forming microheterogeneities in the system.[31−33] It is also possible that glycerol might be partly polymerized under hydrothermal conditions. This gives rise to emulsified spheres serving as soft templates for subsequent deposition of the shell structure. The iron oxide nanoparticles, formed via the hydrolysis of the precursor $FeSO_4 \cdot 7H_2O$, wuold assemble on the surface of these glycerol droplets. During the prolonged hydrothermal treatment, these nanoparticles would crystallize into sheet-like nanostructures, forming robust shells. The inner glycerol quasidroplet is easily removed via solvent extraction during washing while the entire shell is kept intact, leading to formation of a well-defined hollow structure.

The chemical composition of the material is analyzed by X-ray diffraction (XRD), with the result shown in Figure 2A. All the identified diffraction peaks can be unambiguously assigned to the phase-pure rhombohedral Fe_2O_3 (JCPDS card no. 33-0664).[34] The morphology of the sample is further characterized using scanning electron microscopy (SEM; Figure 2B). It shows that the product is composed of spherical particles with a diameter of ~1 μm. It can also be clearly identified that the spheres are actually composed of densely packed sheet-like subunits with relatively small size and thickness. The hollow interior of these spheres is confirmed by transmission electron microscope (TEM) analysis (Figure 2C,D), where they are shown to have a large void space and a well-defined shell. With a closer examination (Figure 2D), the nanosheet subunits can be easily observed. Such an interesting structure renders the sample a high surface area of 103.3 m^2 g^{-1}, with a relatively wide pore size distribution (N_2 adsorption−desorption isotherm of the sample is provided in Supporting Information, Figure S1).

Received: September 4, 2011
Published: October 06, 2011

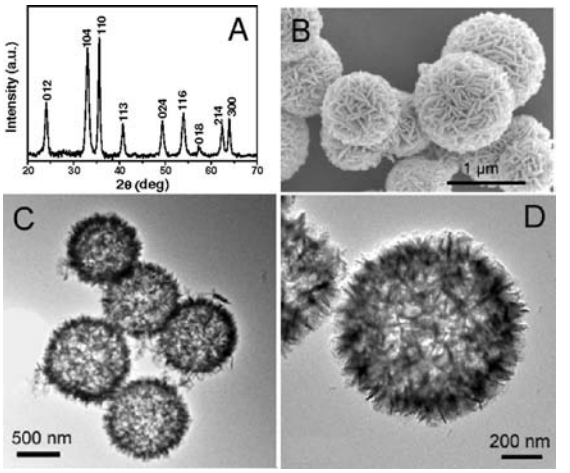

Figure 2. (A) XRD, (B) SEM, and (C,D) TEM images of the α-Fe_2O_3 hierarchical hollow spheres prepared at 145 °C .

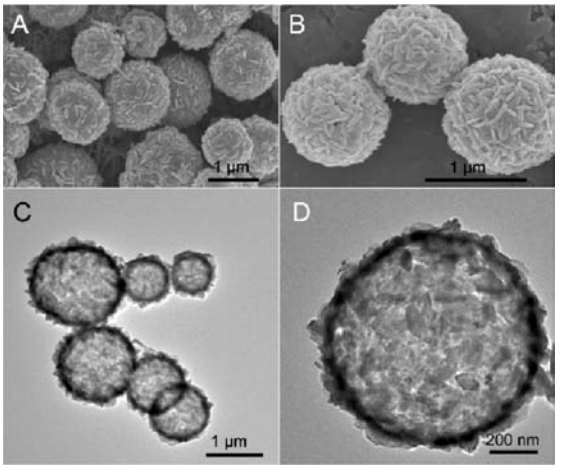

Figure 3. (A,B) SEM and (C,D) TEM images of the α-Fe_2O_3 hierarchical hollow spheres synthesized at a higher temperature of 165 °C, while other conditions remained unchanged.

It is known that the concentration of the soft template has an important influence on the morphology of the product.[28] We thus study the effect of different amounts of glycerol on the structure of the α-Fe_2O_3 hollow spheres. When only 2 mL of glycerol is added into the system, flower-like spherical particles are formed (see Figure S2A). These particles consist of densely packed needle-like subunits, with no internal void space (Figure S2A, inset). On the other hand, if the amount of glycerol used is increased to 8 mL (Figure S2B), the sample contains spherical particles together with a large amount of sheet-like debris. TEM analysis (Figure S2B, inset) confirms the dense packing of these nanosheet subunits, giving the structure an almost solid interior.

We have also carried out experiments under different reaction temperatures. At a lower temperature of 120 °C, urchin-like particles are generated with very thin and long rod-like subunits pointing radially outward (Figure S2C); the TEM image (Figure S2C, inset) confirms that these particles are solid in nature. However, at a higher temperature of 165 °C, spherical particles are again obtained but with a wide size distribution, as shown in Figure 3. It is quite conceivable that, with the increased temperature

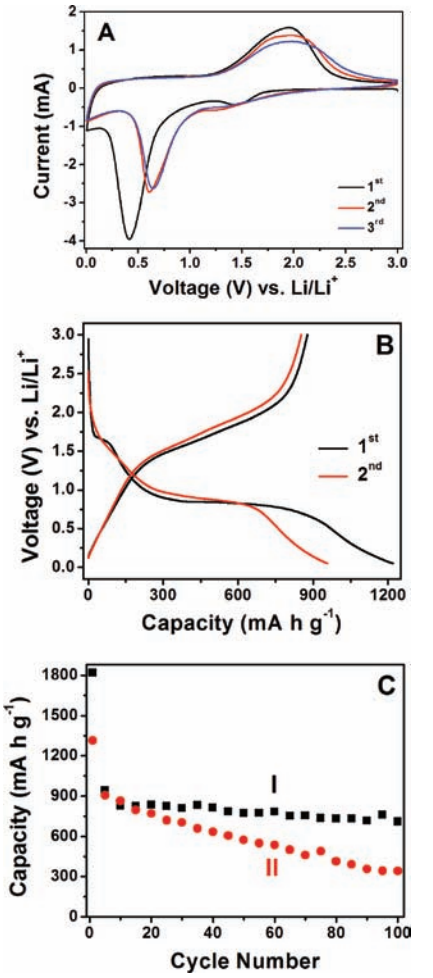

Figure 4. Electrochemical measurements of the sample. (A) CVs between 5 mV and 3 V at a scan rate of 0.5 mV s^{-1}. (B) Charge−discharge voltage profiles. (C) Comparative cycling performance of (I) the as-prepared α-Fe_2O_3 hollow spheres and (II) α-Fe_2O_3 microparticles. All the galvanostatic tests are performed at a constant current rate of 200 mA g^{-1} between 0.05 and 3 V.

and pressure, the glycerol droplets are thermodynamically less stable, considering that no surfactants are used in the system to stabilize the quasimicroemulsion. Thus, it is easier for these droplets to deform into spheres with a wider range of sizes. Under a higher magnification (Figure 3B), it can be observed that these particles are assembled from much smaller nanosheets with a more compact packing. TEM observation again reveals that these spherical particles are hollow, with relatively thin shells (50−100 nm), as shown in Figure 3C,D. The above observations indicate that both the amount of glycerol and the reaction temperature play very important roles in determining the final morphology and structure of the product. If the temperature is further increased to above 180 °C, indeed, hollow α-Fe_2O_3 structures can no longer be formed.

We next study the electrochemical properties of the material. Figure 4A shows the representative cyclic voltammograms (CVs) of the sample between 5 mV and 3 V at a scan rate of 5 mV s^{-1}. Consistent with previous reports,[4,7,12] one pair of distinct redox current peaks can be clearly identified from the CV curves. The reduction peak at ~0.5 V in the cathodic sweep corresponds to the Li insertion into Fe_2O_3 and the formation of Li_2O.

dx.doi.org/10.1021/ja208346s |J. Am. Chem. Soc. 2011, 133, 17146–17148

Apparently, the peak intensity drops significantly in the second cycle, indicating the occurrence of some irreversible processes in the electrode material in the first cycle. On the other hand, the oxidation peak at ~2.0 V in the anodic sweep, attributed to the formation of Fe^{3+} from Fe^0,[4] exhibits little change in the first three cycles, indicating a good reversibility of the electrochemical reaction.

The charge−discharge voltage profiles of the sample are shown in Figure 4B. A distinct voltage plateau can be clearly identified at ~0.75 V, agreeing well with the above CV analysis. This reaction provides the dominant contribution to the Li storage capability of the material, giving rise to a high first-cycle discharge capacity of 1219 mA h g^{-1}. A reversible charge capacity of 877 mA h g^{-1} can be delivered, leading to a relatively low irreversible capacity loss of 28%. The Coulombic efficiency increases rapidly to 89% in the second cycle. The cycling performance of the sample is depicted in Figure 4C, at a constant current density of 200 mA g^{-1} between 0.05 and 3 V. From the second cycle onward, the as-prepared α-Fe_2O_3 hollow spheres exhibit excellent cyclic capacity retention, with a stable capacity of ~750 mA h g^{-1}. At the end of 100 charge−discharge cycles, a reversible capacity as high as 710 mA h g^{-1} can still be retained. As a comparison, the α-Fe_2O_3 microparticles (see Supporting Information, Figure S3) with a comparable size show a much lower first-cycle discharge capacity, and the capacity drops quickly to 340 mA h g^{-1} at the end of the test. Thus, the advantage of as-prepared hollow α-Fe_2O_3 spheres for Li storage is very apparent. Furthermore, when compared to other α-Fe_2O_3-based electrodes tested under similar conditions,[7,12] these unique hierarchical α-Fe_2O_3 hollow spheres manifest greatly enhanced Li storage properties with a higher reversible capacity and a more stable cyclic capacity retention. We could probably attribute this superior performance of our hollow spheres to the thin nanosheet subunits providing a fast and efficient transport of Li ions, and the distinct hollow interior allowing the material to effectively buffer the stress induced during the charge−discharge process.

In summary, α-Fe_2O_3 hollow spheres with sheet-like subunits have been synthesized under hydrothermal conditions via an interesting glycerol/water quasiemulsion-templating mechanism. It is found that synthesis conditions, such as the amount of glycerol and the reaction temperature, have an important influence on the morphology and structure of the product. When tested as the anode material for LIBs, the as-prepared α-Fe_2O_3 hollow spheres exhibit significantly improved Li storage capabilities, with a very high reversible capacity of 710 mA h g^{-1}, even after 100 cycles.

■ ASSOCIATED CONTENT

Ⓢ Supporting Information. Experimental details, N_2 adsorption−desorption isotherm, and more SEM and TEM images. This material is available free of charge via the Internet at http://pubs.acs.org.

■ AUTHOR INFORMATION

Corresponding Author
xwlou@ntu.edu.sg

Author Contributions
[§]These authors contributed equally to this work.

■ ACKNOWLEDGMENT

We are grateful to the National Foundation (Singapore) for financial support through the Clean Energy Research Programme (CERP; NRF2009EWRCERP001-036).

■ REFERENCES

(1) Armand, M.; Tarascon, J. M. *Nature* **2008**, *451*, 652.
(2) Tarascon, J. M.; Armand, M. *Nature* **2001**, *414*, 359.
(3) Chen, J. S.; Archer, L. A.; Lou, X. W. *J. Mater. Chem.* **2011**, *21*, 9912.
(4) Chen, J.; Xu, L. N.; Li, W. Y.; Gou, X. L. *Adv. Mater.* **2005**, *17*, 582.
(5) Chen, J. S.; Li, C. M.; Zhou, W. W.; Yan, Q. Y.; Archer, L. A.; Lou, X. W. *Nanoscale* **2009**, *1*, 280.
(6) Chen, J. S.; Zhu, T.; Yang, X. H.; Yang, H. G.; Lou, X. W. *J. Am. Chem. Soc.* **2010**, *132*, 13162.
(7) Nuli, Y. N.; Zhang, P.; Guo, Z. P.; Liu, H. K. *J. Electrochem. Soc.* **2008**, *155*, A196.
(8) Zhang, W. M.; Wu, X. L.; Hu, J. S.; Guo, Y. G.; Wan, L. J. *Adv. Funct. Mater.* **2008**, *18*, 3941.
(9) Wang, Z.; Luan, D.; Madhavi, S.; Li, C. M.; Lou, X. W. *Chem. Commun.* **2011**, *47*, 8061.
(10) Zeng, S. Y.; Tang, K. B.; Li, T. W.; Liang, Z. H.; Wang, D.; Wang, Y. K.; Qi, Y. X.; Zhou, W. W. *J. Phys. Chem. C* **2008**, *112*, 4836.
(11) Pan, Q. T.; Huang, K.; Ni, S. B.; Yang, F.; Lin, S. M.; He, D. Y. *J. Phys. D: Appl. Phys.* **2009**, 42.
(12) Kim, H. S.; Piao, Y.; Kang, S. H.; Hyeon, T.; Sung, Y. E. *Electrochem. Commun.* **2010**, *12*, 382.
(13) Zhou, J. S.; Song, H. H.; Chen, X. H.; Zhi, L. J.; Yang, S. Y.; Huo, J. P.; Yang, W. T. *Chem. Mater.* **2009**, *21*, 2935.
(14) Wu, C. Z.; Yin, P.; Zhu, X.; OuYang, C. Z.; Xie, Y. *J. Phys. Chem. B* **2006**, *110*, 17806.
(15) Fei, J.; Cui, Y.; Zhao, J.; Gao, L.; Yang, Y.; Li, J. *J. Mater. Chem.* **2011**, *21*, 11742.
(16) Xu, J.-S.; Zhu, Y.-J. *CrystEngComm* **2011**, *13*, 5162.
(17) Zhong, L. S.; Hu, J. S.; Liang, H. P.; Cao, A. M.; Song, W. G.; Wan, L. J. *Adv. Mater.* **2006**, *18*, 2426.
(18) Choi, W. S.; Koo, H. Y.; Zhongbin, Z.; Li, Y.; Kim, D. Y. *Adv. Funct. Mater.* **2007**, *17*, 1743.
(19) Lou, X. W.; Archer, L. A.; Yang, Z. C. *Adv. Mater.* **2008**, *20*, 3987.
(20) Bao, J. C.; Liang, Y. Y.; Xu, Z.; Si, L. *Adv. Mater.* **2003**, *15*, 1832.
(21) Buchold, D. H. M.; Feldmann, C. *Nano Lett.* **2007**, *7*, 3489.
(22) Fowler, C. E.; Khushalani, D.; Mann, S. *Chem. Commun.* **2001**, 2028.
(23) Han, J.; Song, G. P.; Guo, R. *Adv. Mater.* **2006**, *18*, 3140.
(24) Hu, Y.; Chen, J. F.; Chen, W. M.; Lin, X. H.; Li, X. L. *Adv. Mater.* **2003**, *15*, 726.
(25) Imhof, A.; Pine, D. J. *Nature* **1997**, *389*, 948.
(26) Jovanovic, A. V.; Underhill, R. S.; Bucholz, T. L.; Duran, R. S. *Chem. Mater.* **2005**, *17*, 3375.
(27) Wang, H.; Song, Y.; Medforth, C. J.; Shelnutt, J. A. *J. Am. Chem. Soc.* **2006**, *128*, 9284.
(28) Yang, H. G.; Zeng, H. C. *Angew. Chem., Int. Ed.* **2004**, *43*, 5206.
(29) Yu, X. L.; Cao, C. B.; Zhu, H. S.; Li, Q. S.; Liu, C. L.; Gong, Q. H. *Adv. Funct. Mater.* **2007**, *17*, 1397.
(30) Zoldesi, C. I.; Imhof, A. *Adv. Mater.* **2005**, *17*, 924.
(31) Ruckenstein, E.; Shulgin, I. *Chem. Eng. Sci.* **2001**, *56*, 5675.
(32) Roney, A. B.; Space, B.; Castner, E. W.; Napoleon, R. L.; Moore, P. B. *J. Phys. Chem. B* **2004**, *108*, 7389.
(33) Idrissi, A.; Longelin, S. *J. Mol. Struct.* **2003**, *651*, 271.
(34) Chen, J. S.; Zhu, T.; Li, C. M.; Lou, X. W. *Angew. Chem., Int. Ed.* **2011**, *50*, 650.